Electronic Supplementary Information: Integration of Nanoporous Membranes in Microfluidic Devices: Electrokinetic Bio-sample Pre-concentration

Minseok Kim and Taesung Kim*

CORRESPONDENCE: tskim@unist.ac.kr

SECTIONS

1. **Fluid-patterning process using dual-depth microfluidic channels**

2. **Solidification process of the Nafion membrane**

3. **Solidification process of the poly-HEMA membrane**

4. **Chemical compatibility of the membranes**

5. **Ionic current measurement of the membranes**

6. **Influence of pressure driven flow (PDF) on pre-concentration**

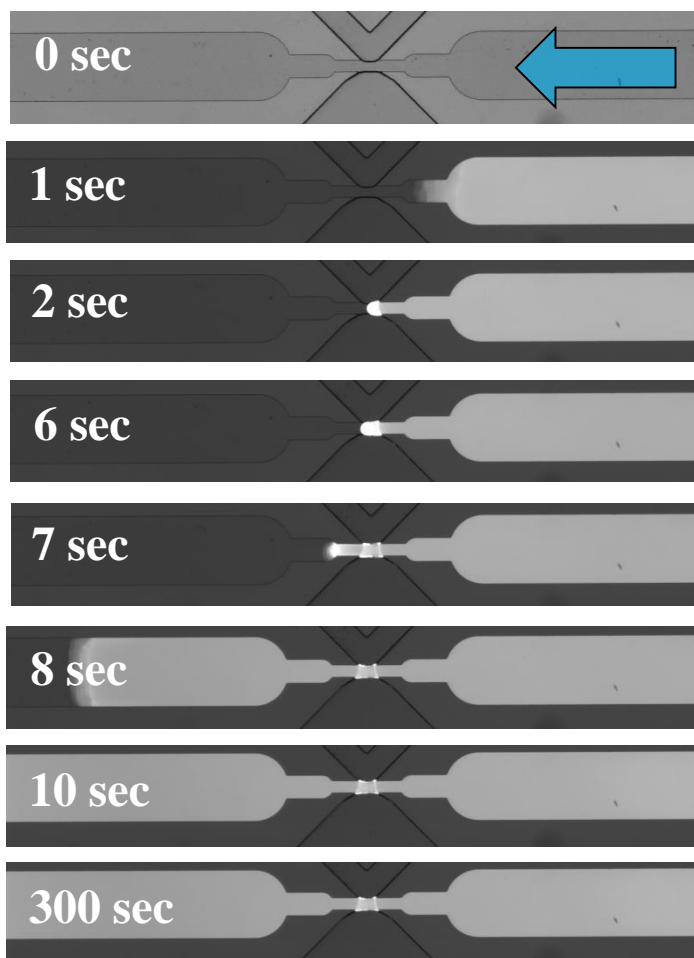**1. Fluid-patterning process using dual-depth microfluidic channels**

Figure S1 Time-lapse fluorescent images of the fluid filling process. A fluorescent dye (FITC) containing DI water was loaded from the right side of the shallow channel. The fluid passes through the junction in 7 sec and then arrives at the left channel in 8 sec only along the shallow channel. Although the fluid patterning process highly depends on the viscosity of the fluid, the patterned fluid maintained its shape for a long time (over 300 sec) for which solidification process can be completed.

2. Solidification process of the Nafion membrane

1 min

Cured Nafion

Shrinking direction of persecutor

2 min

Cured Nafion

3 min

Cured Nafion

4 min
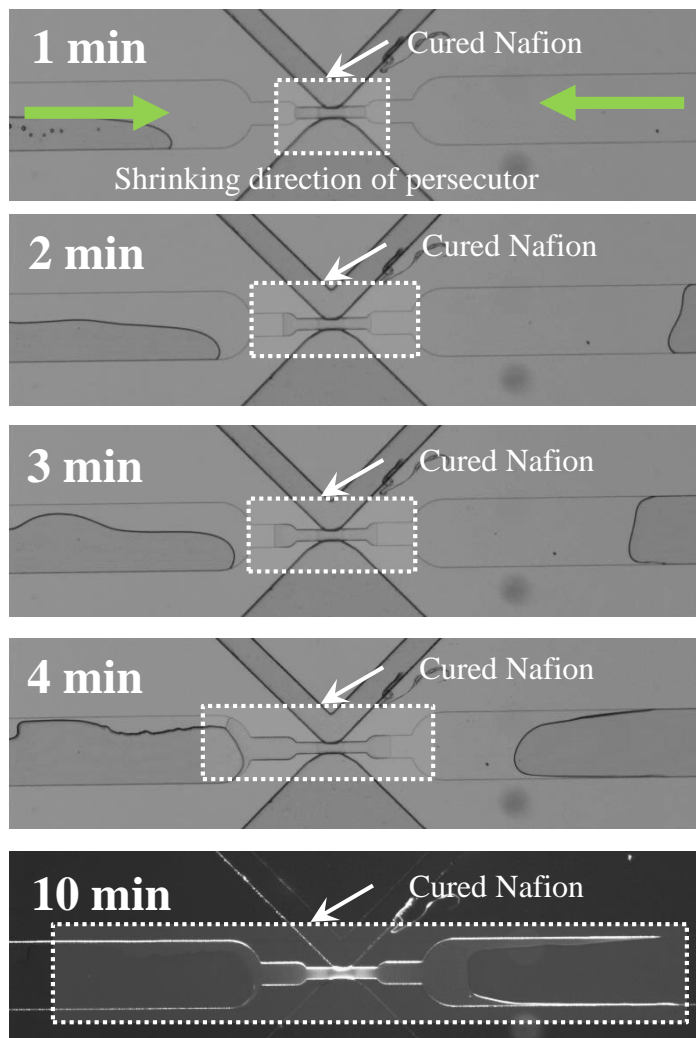
Cured Nafion

10 min

Cured Nafion

Figure S2 Time-lapse images of solidification process of the Nafion membrane. The Nafion precursor solution on 95 °C hotplate starts to be solidified from the junction and then expands along the shallow channel because solvents in the solution gradually evaporate away through the deep channels.

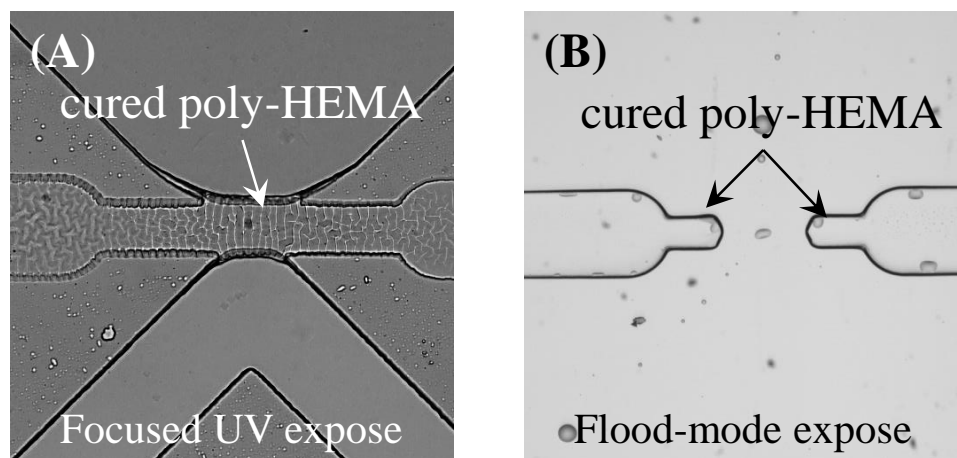## 3. Solidification process of the poly-HEMA membrane

Figure S3 A difference between focused UV irradiation and flood mode UV irradiation for the photo-curing process of the poly-HEMA. (A) The focused UV irradiation initiates photo-polymerization of the poly-HEMA from the junction while (B) the flood-mode UV initiates photo-polymerization from the enlarged area and around reservoirs of the shallow channel. For the former photo-curing process, volume contraction was replenished with extra precursor solutions in the enlarged channel area. On the other hand, for the latter case, volume contraction in the large channels seems to be stronger than that in the junction, resulting in that a tight-sealed membrane was not successfully fabricated.

4. Chemical compatibility of the membranes

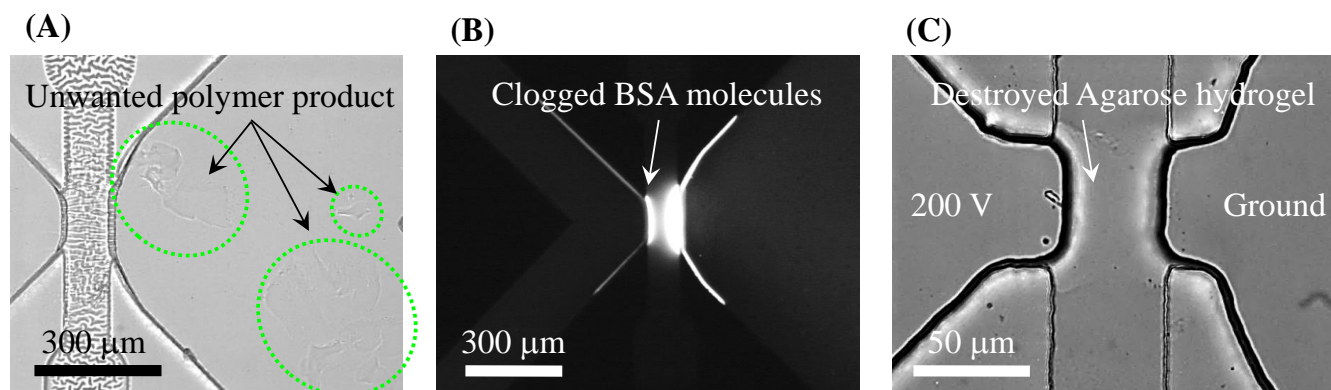**(A)**   **(B)**   **(C)**

Figure S4 (A) The poly-HEMA with AA show unstable behavior in a PBS buffer solution (1 mM) but they are successfully solidified in a KCl buffer solution (1 mM). (B) The poly-HEMA with DMAEMA show clogging problems with negatively charged protein (BSA). This can be attributed to the surface charge density of the membrane, electrostatically attracting negatively charged proteins. (C) The agarose hydrogel is damaged in the present of a strong electric field (200 V/cm). This can be attributed to the Joule heating and a high pressure build-up.

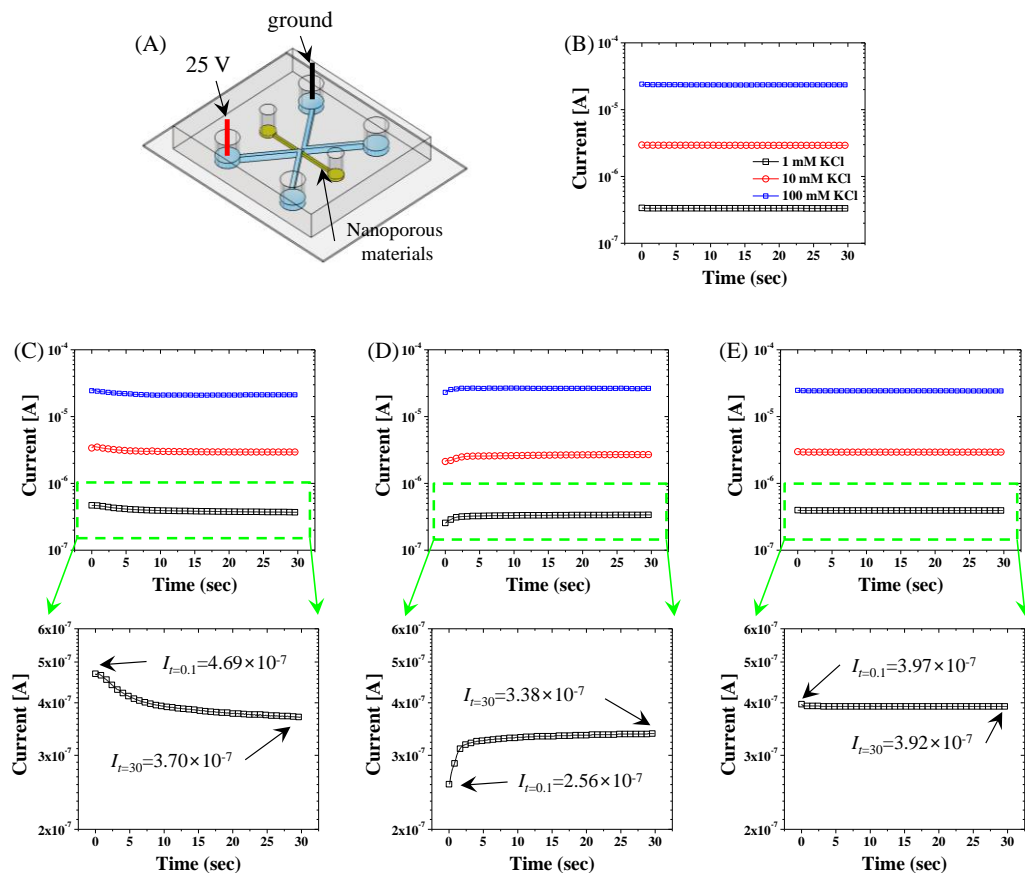## 5. Ionic current measurement of the membranes

Figure S5 Measurement of ionic current profiles. (A) The schematic illustration shows the experimental setup for measuring relative permselectivity that depends on integrated membranes, electric potentials, buffer strengths and so on. (B) The current profiles of a membrane-free microchannel show no notable current differences between a starting and a steady state point. (C)–(E) The current profiles of NPM-integrated microchannels are presented: (C) poly-HEMA with AA, (D) poly-HEMA with DMAEMA, and (E) argarose hydrogel, respectively. The HEMA mixtures show decaying current profiles while the agarose current profiles that are very close to those of the membrane-free microchannel for 1 mM, 10 mM and 100 mM KCl buffer solutions.

6. Influence of pressure driven flow (PDF) on pre-concentration

To facilitate the concentration rate in the fixed electrokinetic configuration, we applied additional PDFs (5 pl/s and 10 pl/s) to increase the sample delivery rate in the anodic channel. The additional PDFs were simply controlled by breaking the balance of hydraulic heights between two sample reservoirs. Because applying high electric potential and changing the electric configuration are often limited depending on a sample condition, additional sample delivery based on PDF is an efficient and easy way to control. It should be emphasized that the enhancement of the sample concentration rate using the additional PDF is possible because the device have large effective surface area for permselective mass transport (50 μm × 15 μm). The larger effective surface area allows more rapid ionic flux through the NPMs so that the depletion area can be stably maintained even in fairly large PDF rates. On the other hand, nano-thick nanojunctions (<1 μm) have limited mass transport area such that the additional PDF to increase the concentration rate would lead unstable sample accumulation. Consequently, the concentrated sample would be flow away to the lower pressure reservoir due to the high PDF rate, meaning unstable sample concentration.
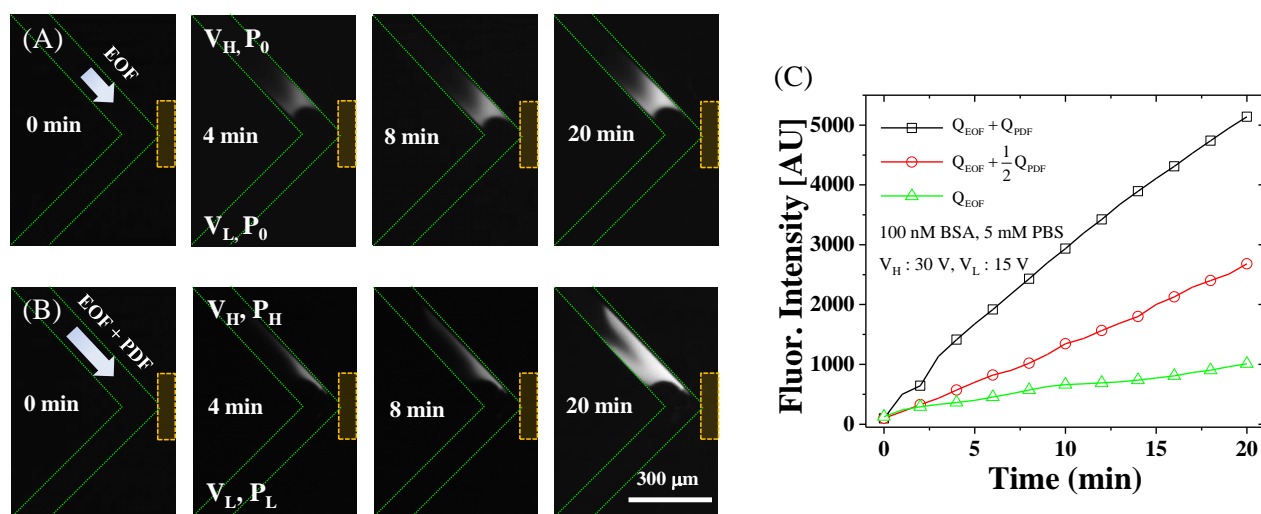

Figure S6 Enhancement of concentration rate by additional pressure driven flow (PDF) to EOF. (A) shows time sequential images of biomolecule concentration by the external electric field (V_H-V_L) and (B) shows the concentration enhancement by the additional potential gradient (P_H-P_L). Because of the high capability of the device to strongly maintain depletion area, additional bulk flow by pressure difference improves the pre-concentration rate. (C) Shows the quantitative result of the microscopic images.